ORIGINAL ARTICLE

JBMR®

Disruption of *Scube2* Impairs Endochondral Bone Formation

Yuh-Charn Lin,[1,2] Steve R. Roffler,[2] Yu-Ting Yan,[2] and Ruey-Bing Yang[1,2,3]

[1]Graduate Institute of Life Sciences, National Defense Medical Center, Taipei, Taiwan
[2]Institute of Biomedical Sciences, Academia Sinica, Taipei, Taiwan
[3]Institute of Pharmacology, School of Medicine, National Yang-Ming University, Taipei, Taiwan

ABSTRACT

Signal peptide-CUB-EGF domain-containing protein 2 (SCUBE2) belongs to a secreted and membrane-tethered multidomain SCUBE protein family composed of three members found in vertebrates and mammals. Recent reports suggested that zebrafish *scube2* could facilitate sonic hedgehog (*Shh*) signaling for proper development of slow muscle. However, whether SCUBE2 can regulate the signaling activity of two other hedgehog ligands (*Ihh* and *Dhh*), and the developmental relevance of the SCUBE2-induced hedgehog signaling in mammals remain poorly understood. In this study, we first showed that as compared with SCUBE1 or SCUBE3, SCUBE2 is the most potent modulator of IHH signaling in vitro. In addition, gain and loss-of-function studies demonstrated that SCUBE2 exerted an osteogenic function by enhancing *Ihh*-stimulated osteoblast differentiation in the mouse mesenchymal progenitor cells. Consistent with these in vitro studies and the prominent roles of *Ihh* in coordinating skeletogenesis, genetic ablation of *Scube2* (–/–) caused defective endochondral bone formation and impaired *Ihh*-mediated chondrocyte differentiation and proliferation as well as osteoblast differentiation of –/– bone-marrow mesenchymal stromal-cell cultures. Our data demonstrate that *Scube2* plays a key regulatory role in *Ihh*-dependent endochondral bone formation. © 2015 American Society for Bone and Mineral Research.

KEY WORDS: HEDGEHOGS; GENETIC ANIMAL MODELS; MOLECULAR PATHWAYS–DEVELOPMENT; OSTEOBLAST; BONE μCT

Introduction

Signal peptide–complement protein C1r/C1s, Uegf, and Bmp1 (CUB)–epidermal growth factor (EGF) domain-containing protein 2 (*SCUBE2*) is the second member of a newly identified SCUBE gene family that has been evolutionarily conserved from zebrafish to humans.[1–10] Three different human genes (*SCUBE1*, *SCUBE2*, and *SCUBE3*) have been described. They encode polypeptides of approximately 1000 amino acids organized in a modular fashion with five protein domains: an NH_2-terminal signal peptide sequence; nine tandem repeats of EGF-like motifs; a large spacer N-glycosylated region; three cysteine-rich repeats; and one CUB domain at the COOH terminus.[1,11] When overexpressed, recombinant SCUBE2 protein forms oligomers that are secreted into the conditioned medium or remain tethered on the cell surface, where it behaves like a peripheral membrane (not membrane-spanning) protein.[1,2] Thus, SCUBE2 may function differently depending on its expression as a soluble or surface-associated protein.

Mouse *Scube2* is expressed in embryonic neuroectoderm, developing face, heart, and the perichondrium of endochondral skeletal structures, including developing ribs, lumbar vertebrae, and long bones of limbs.[7,12] The perichondrium, composed of undifferentiated mesenchymal cells surrounding growth-plate cartilage, differentiates into osteoblasts that populate future cortical and trabecular bone.[13,14] However, whether *Scube2* is involved in endochondral bone formation or other developmental processes remains largely unknown in mammals.

Zebrafish genetic studies suggested that *scube2* is essential for proper hedgehog (HH) signaling in development of slow muscle and ventral spinal cord fates.[8–10] The HH signaling pathway, originally found in *Drosophila*, is also conserved in vertebrates. The fly has only one HH, whereas the mammalian HH family consists of three protein ligands—sonic (SHH), Indian (IHH), and desert (DHH)—involved in embryonic development of multiple tissues and organs.[15,16] For example, prenatal IHH, expressed mainly in prehypertrophic chondrocytes, acts in coordinating chondrocyte proliferation and differentiation and signals perichondrial mesenchymal cells to differentiate into osteoblasts during skeletal development.[17–21] Postnatally, chondrocyte-derived IHH is essential for maintaining growth plate and sustaining trabecular bone and skeletal growth.[22]

In agreement with zebrafish genetic studies, we and others recently demonstrated that SCUBE2 can positively regulate SHH signaling via two distinctive modes of action. First, the soluble form of SCUBE2 can act on the ligand-producing cells to

Received in original form August 27, 2014; revised form December 17, 2014; accepted January 5, 2015. Accepted manuscript online January 12, 2015.
Address correspondence to: Ruey-Bing Yang, PhD, Institute of Biomedical Sciences, Academia Sinica, Taipei 115, Taiwan.
E-mail: rbyang@ibms.sinica.edu.tw
Additional Supporting Information may be found in the online version of this article.
Journal of Bone and Mineral Research, Vol. 30, No. 7, July 2015, pp 1255–1267
DOI: 10.1002/jbmr.2451

facilitate the release (possibly as protease enhancers) and solubilization of dual-lipidated SHH ligand for distant signaling.[23–25] In addition, membrane-anchored SCUBE2 within the raft microdomains can bind, concentrate, and facilitate the presentation of SHH to the PTCH1 receptor in signal responding cells.[1] However, whether SCUBE2 could also modulate the signaling activity of other HH ligands remains largely unknown. Most importantly, the developmental importance of SCUBE2-enhanced HH signaling in vivo has not been formally addressed.

In this study, we first showed that as compared with SCUBE1 or SCUBE3, SCUBE2 is the most active modulator for IHH signaling in vitro. In agreement with our in vitro studies and the predominant roles of *Ihh* in regulating skeletogenesis,[26] genetic ablation of *Scube2* impaired *Ihh*-dependent chondrocyte differentiation and proliferation as well as osteoblast differentiation during endochondral ossification in mice. Thus, SCUBE2 may be a key regulator in *Ihh*-mediated endochondral bone formation.

Materials and Methods

Cells and transfection

C3H/10T1/2, NIH/3T3, and Shh-LIGHT2 mouse embryo fibroblasts were from the American Type Culture Collection (Manassas, VA, USA). Human embryonic kidney (HEK)-293T cells or Shh-LIGHT2 cells were transfected by use of Lipofectamine 2000 (Life Technologies, Grand Island, NY, USA) or FuGENE HD (Promega, Madison, WI, USA), respectively.

Gli (glioma-associated oncogene/zinc finger protein family)-dependent luciferase reporter assay

Assays for HH-pathway activation in Shh-LIGHT2 cells, an NIH/3T3 cell line stably incorporating firefly luciferase and constitutive *Renilla* luciferase reporters, were as described.[27]

Western blot analysis

Primary antibodies were anti-SCUBE2 (GeneTex, Irvine, CA, USA), anti-HH, and anti-osteocalcin (Santa Cruz Biotechnology, Santa Cruz, CA, USA). Secondary antibodies were horseradish peroxidase-conjugated goat anti-rabbit or anti-mouse IgG (Jackson ImmunoResearch Laboratories, West Grove, PA, USA).

Lentiviral preparation and infection

C3H/10T1/2 cells were engineered with the full-length SCUBE2 expression vector or empty vector (control) by a self-inactivating lentiviral transduction system.[28] We used the vector-based short hairpin RNAs (shRNAs) generated by The RNAi Consortium[29] to knock down the endogenous SCUBE2 in the C3H/10T1/2 cell line. Lentiviral infection involved incubating the desired amount of virus preparation with C3H/10T1/2 cells in culture, typically 0.5 mL per 5×10^5 cells, for 12 hours, then the medium was changed.

RNA extraction and gene expression analysis

Total RNA was obtained from cultured cells by the TRIzol method (Life Technologies, Grand Island, NY, USA). First-strand cDNA synthesis with SuperScript II reverse transcriptase (Life Technologies) involved 5 μg RNA. One-tenth of the first-strand cDNA reaction was used for each PCR as a template. Primers are listed in Supporting Table 1.

Determination of alkaline phosphatase activity

Cells were washed with phosphate buffered saline and lysed with 0.05% Triton X-100 solution. Alkaline phosphatase (ALP) activity in lysates was determined with *p*-nitrophenol-phosphate used as a substrate.[30]

Generation of *Scube2* knockout (–/–) mice

The targeting vector (as described in Supporting Fig. S1) was electroporated into the mouse embryonic stem (ES) cell R1 line. The correctly targeted ES cell clones were injected into blastocysts and implanted into pseudopregnant C57BL/6 females. Heterozygous global $Scube2^{+/-}$ (+/–) mice were generated by crossing male protamine (Prm)-Cre;[31] $Scube2^{Flox/+}$ mice to wild-type (WT) female mice. The targeted allele was backcrossed with C57BL/6 females for at least six generations before experiments. Mice homozygous for the WT (+/+) allele or null (–/–) allele were obtained by interbreeding +/– offspring and verified by PCR. All experimental procedures were approved by the Institutional Animal Care and Utilization Committee at Academia Sinica, Taiwan. Only male mice (+/+ or –/–) were used for this study. In addition, $n = 5$ (or more as indicated) animals in each genotype group were used for all phenotyping analyses.

Radiography, micro–computed tomography, and bone densitometry

Radiography and 3D reconstructed CT images were obtained by scanning calcified bone by micro–computed tomography (μCT) (Skyscan 1076; Skyscan, Antwerp, Belgium) at 50 kV, 200 mA, 0.4-degree rotation, 0.5-mm Al filter, and 9-mm/pixel scan resolution. Bone mineral density (BMD) analysis was at 50 kV, 200 mA, 1-degree rotation, 0.5-mm Al filter, and 35-μm/pixel scan resolution. Cross-sections were reconstructed by using a cone-beam algorithm (software Cone_rec; Skyscan). Files were imported into CTAn software (Skyscan) for 3D analysis and image generation. BMD for each femur was measured by use of CTAn, by calibration with phantoms with known BMD (0.25 to 0.75 g/cm^3).

Dual calcein labeling for measurement of dynamic bone formation rate

In vivo double labeling with calcein was performed as described.[32] Six-week-old –/– mice and +/+ littermates were injected subcutaneously with calcein (25 mg/kg body weight) 13 days and 3 days before euthanasia. Femur specimens were harvested and fixed in formal saline. Undecalcified bone sections (10-μm-thick) on glass slides were used to examine double-labeled fluorescence under a fluorescence microscope.

Alizarin red/Alcian blue staining of skeleton

Bone and cartilage of –/– newborns and +/+ littermates were stained with Alizarin red S (Sigma) or Alcian blue (Sigma) as described.[33]

Primary mouse bone marrow stromal cell culture and Alizarin red S staining

Bone marrow stromal cells (BMSCs) were obtained from 4-week-old –/– mice and +/+ littermates as described.[34] At late osteogenic differentiation, calcium deposition was quantified by Alizarin red S staining. Briefly, cultured cells were washed with cold phosphate-buffered saline, fixed for 15 min in 10% formalin, and stained with 40 mM Alizarin red S solution for 20 min. Stained cells were washed with deionized water to remove the nonspecific precipitation. Positive red staining represented

calcium deposits on the cells. Photographs were obtained for analysis of late-stage osteogenic differentiation. Matrix mineralization was quantified by extracting the Alizarin red S staining with 100 mM cetylpyridinium chloride at room temperature for 3 hours. The absorbance of the extracted Alizarin red S stain was measured at 570 nm.

Statistical analyses

Data are mean ± SD and analyzed by two-tailed paired *t* tests. A value of $p < 0.05$ was considered statistically significant.

Results

Scube2 is the most effective enhancer for IHH signaling and is involved in IHH-dependent osteoblast differentiation

To evaluate the effects of SCUBE members on the signaling activity of each HH ligand, we cotransfected expression plasmids encoding each SCUBE member with the expression construct encoding IHH, SHH, or DHH in Shh-LIGHT2 cells, an NIH/3T3-derived cell line that responds to HH ligands by activating an integrated Gli-dependent firefly luciferase and control *Renilla* luciferase reporter[27] (Fig. 1*A*). Expression of each HH ligand alone could increase Gli-dependent luciferase reporter activity by twofold to fivefold as compared with the empty vector (Fig. 1*B*); however, coexpression of SCUBE2 further enhanced the HH-induced transcriptional activation by an additional 1.6-fold to 3.4-fold. SCUBE2 had the greatest effect on facilitating the signaling activity of IHH as compared with SHH or DHH (3.4-fold versus 1.6-fold; Fig. 1*B*). A similar result was independently verified in HeLa cells (Supporting Fig. S1).

Because overexpressed SCUBE2 manifested as a soluble or cell surface-tethered protein,[1,2] we examined whether SCUBE2-enhanced IHH signaling was attributed to its soluble form. We first harvested soluble SCUBE proteins in conditioned medium with HEK-293T cells overexpressing each SCUBE member (Fig. 2*A*, *B*), then added this medium (after ultracentrifugation at 100,000 g for 2 hours to sediment the membrane-associated but not soluble protein) to NIH/3T3 cells stably expressing IHH or SHH (Fig. 2*A*, *B*). In agreement with the cotransfection experiments (Fig. 1), the addition of soluble SCUBE2 increased the amount of secreted IHH and SHH protein in the medium and prominently enhanced the signaling activity of medium incubated with cells expressing IHH or SHH (Fig. 2*C*, *D*). Again, we observed a greater effect of soluble SCUBE2 on augmenting the signaling activity of IHH by increasing its secretion as compared with SHH (4.3-fold versus 2.4-fold) (Fig. 2*D*). Interestingly, coimmunoprecipitation experiments demonstrated that SCUBE2 can form a complex with IHH ligand and its receptor PTCH1, suggesting that SCUBE2 may facilitate IHH signaling or enhance IHH secretion through these direct molecular interactions (Supporting Fig. S2).

Because genetic and cell biological studies demonstrated that IHH plays important roles in bone development and osteoblast differentiation[17,19,35,36] and our results showed that SCUBE2 can increase IHH signaling activity (Figs. 1 and 2), we then examined the effect of SCUBE2 on IHH-stimulated osteoblast differentiation by measuring the induced activity of ALP, a marker of osteoblast differentiation, in the mouse mesenchymal progenitor cell line C3H10T1/2. Ectopic SCUBE2 overexpression in C3H10T1/2 cells as compared to SCUBE1 or SCUBE3 overexpression had the greatest effect on IHH-promoted ALP activity (Fig. 3*A*, *B*). To further confirm

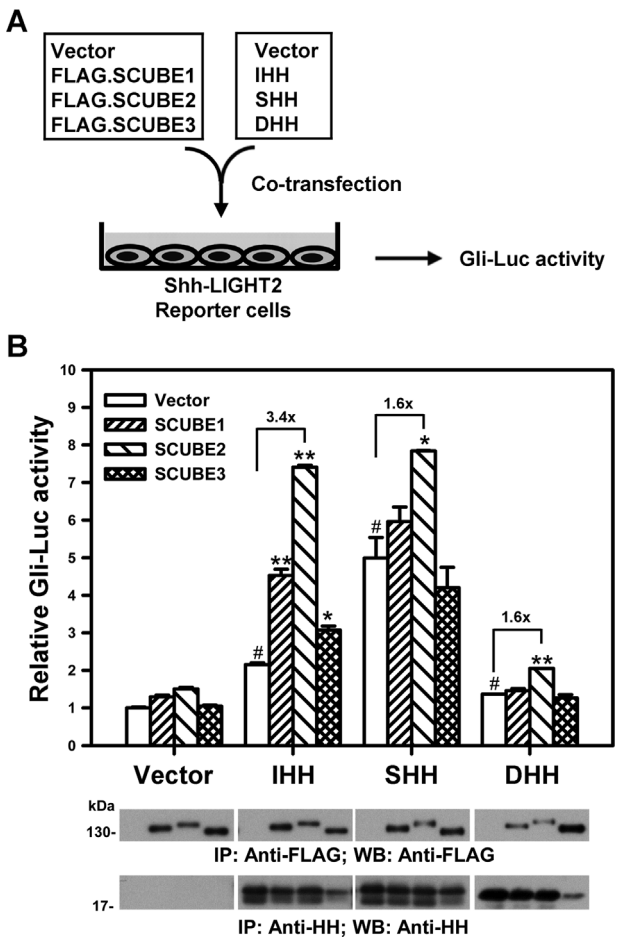

Fig. 1. SCUBE2 is the most potent enhancer for IHH signaling. (*A*) Experimental scheme to test the effects of different SCUBE proteins on HH signaling. Shh-LIGHT2 reporter cells (Shh-responsive cells stably incorporating Gli-dependent firefly luciferase and constitutive *Renilla* luciferase reporters) transfected with an empty vector or the expression plasmid encoding FLAG-tagged SCUBE1, SCUBE2, or SCUBE3 along with an empty vector or an expression construct encoding IHH, SHH, or DHH. Two days after transfection, HH signal activity was measured and reflected as Gli-Luc reporter activity. (*B*) SCUBE2 promotes HH signaling, with a stronger effect on IHH than with SHH or DHH. The experiments were performed three times in triplicate with similar results. Data are mean ± SD relative luciferase activity (firefly luciferase/*Renilla* internal control). Note that each HH protein can induce a significant Gli-Luc activity as compared to the vector control (#$p < 0.05$). *$p < 0.05$, **$p < 0.01$ compared to the vector control. Comparable expression of SCUBE and HH protein was verified by Western blot analysis (bottom panel).

the osteogenic role of *Scube2*, we used two independent *Scube2*-targeting short hairpin RNA lentiviruses (SCUBE2-shRNA #1 and #2) to inhibit endogenous *Scube2* expression in C3H10T1/2 cells. As a negative control, cells were infected with an shRNA lentivirus targeting bacterial β-galactosidase (control shRNA). The efficiency and specificity of shRNA-mediated knockdown of mRNA expression of *Scube2* (but not *Scube1* and *Scube3*) were verified by RT-PCR analysis (Fig. 3*D*). IHH-induced ALP activity was concomitantly suppressed with *Scube2* knockdown (Fig. 3*E*). Furthermore, the expression of osteogenic marker genes Runt-related transcription factor 2 (*Runx2*, a transcriptional activator of

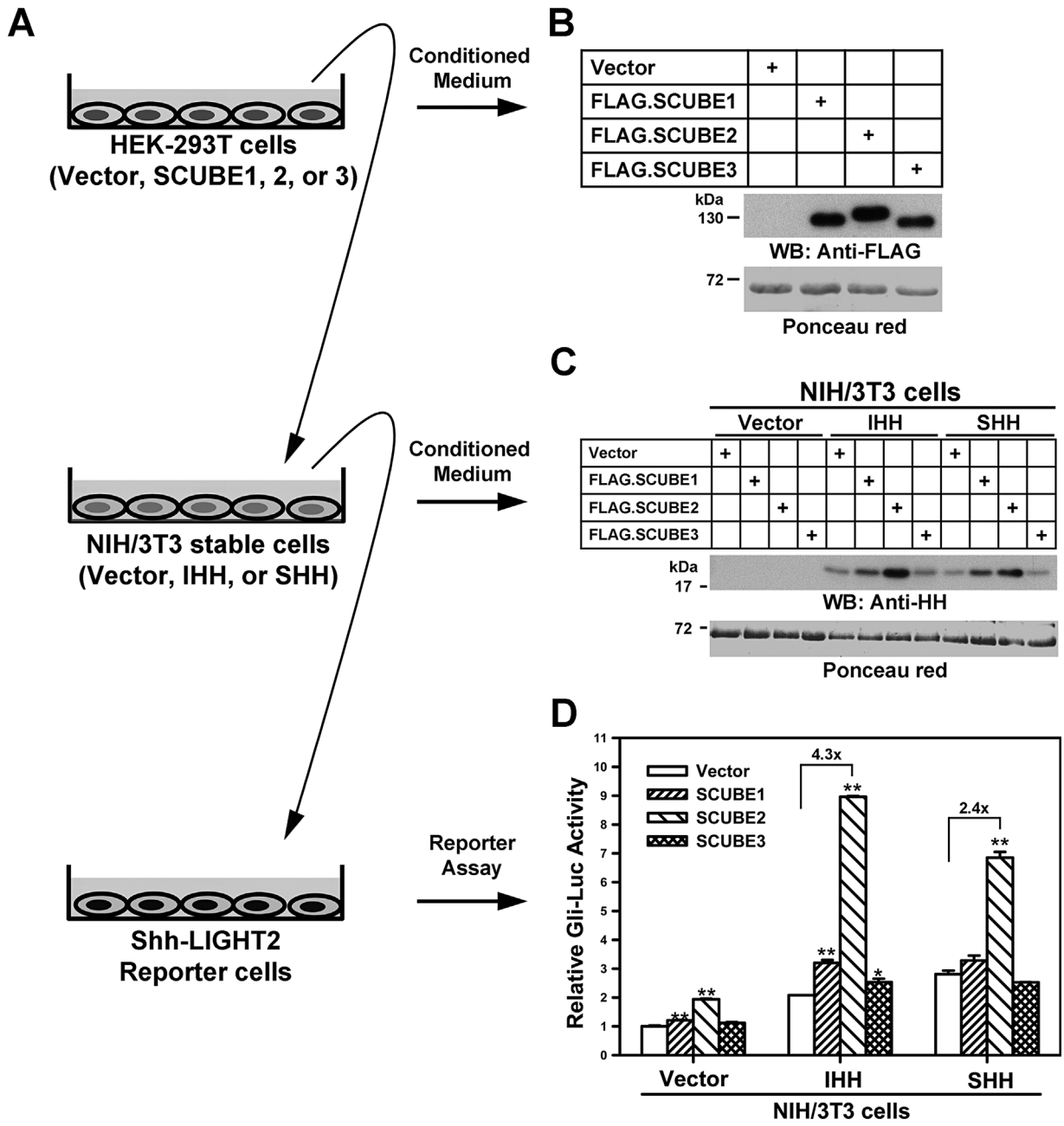

Fig. 2. Secreted SCUBE2 protein enhances the release and mobilization of HH protein for long-range signaling. (*A*) Experimental scheme to test for the effects of secreted SCUBE proteins on the release of HH. HEK-293T cells were transfected with an empty vector (Vector) or the expression plasmid encoding the FLAG-tagged SCUBE1, SCUBE2, or SCUBE3 protein (top panel). Two days after transfection, the conditioned media from Vector-transfected, SCUBE1-transfected, SCUBE2-transfected, or SCUBE3-transfected cells was centrifuged at 100,000*g* for 2 hours and added to cultured medium of the empty vector (Vector)-expressing, IHH-expressing, or SHH-expressing stable NIH/3T3 cells for 2 days (middle panel). HH-conditioned medium was centrifuged at 100,000*g* for 2 hours. Activity was measured in Shh-LIGHT2 reporter cells and twofold dilution of conditioned medium with DMEM containing 0.5% fetal bovine serum (bottom panel). (*B*) Production of soluble SCUBE protein. Conditioned media from HEK-293T cells transduced with vector or SCUBE expression plasmid was immunoblotted with anti-FLAG antibody to verify the comparable expression of secreted SCUBE protein (FLAG-tagged). Ponceau red staining of membranes confirmed relative loading of total proteins for each sample. (*C*) Secreted SCUBE2 stimulates the release of HH proteins. HH-expressing cells were incubated with vector or SCUBE-containing conditioned media. SCUBE2-containing conditioned media increased the release of HH proteins, as detected by anti-HH immunoblotting. Ponceau red staining of membranes confirmed the relative loading of total proteins for each sample. (*D*) Signaling activities of the released HH proteins in conditioned media from HH-expressing cells. After incubation for 2 days with Shh-LIGHT2 cells, relative reporter activity (firefly luciferase/*Renilla* internal control) was normalized to relative reporter activity produced by media collected from NIH/3T3 cells transduced with an empty vector cultured in the absence of SCUBE protein. All assays were performed three times with similar results. Data are mean ± SD. $*p < 0.05$, $**p < 0.01$.

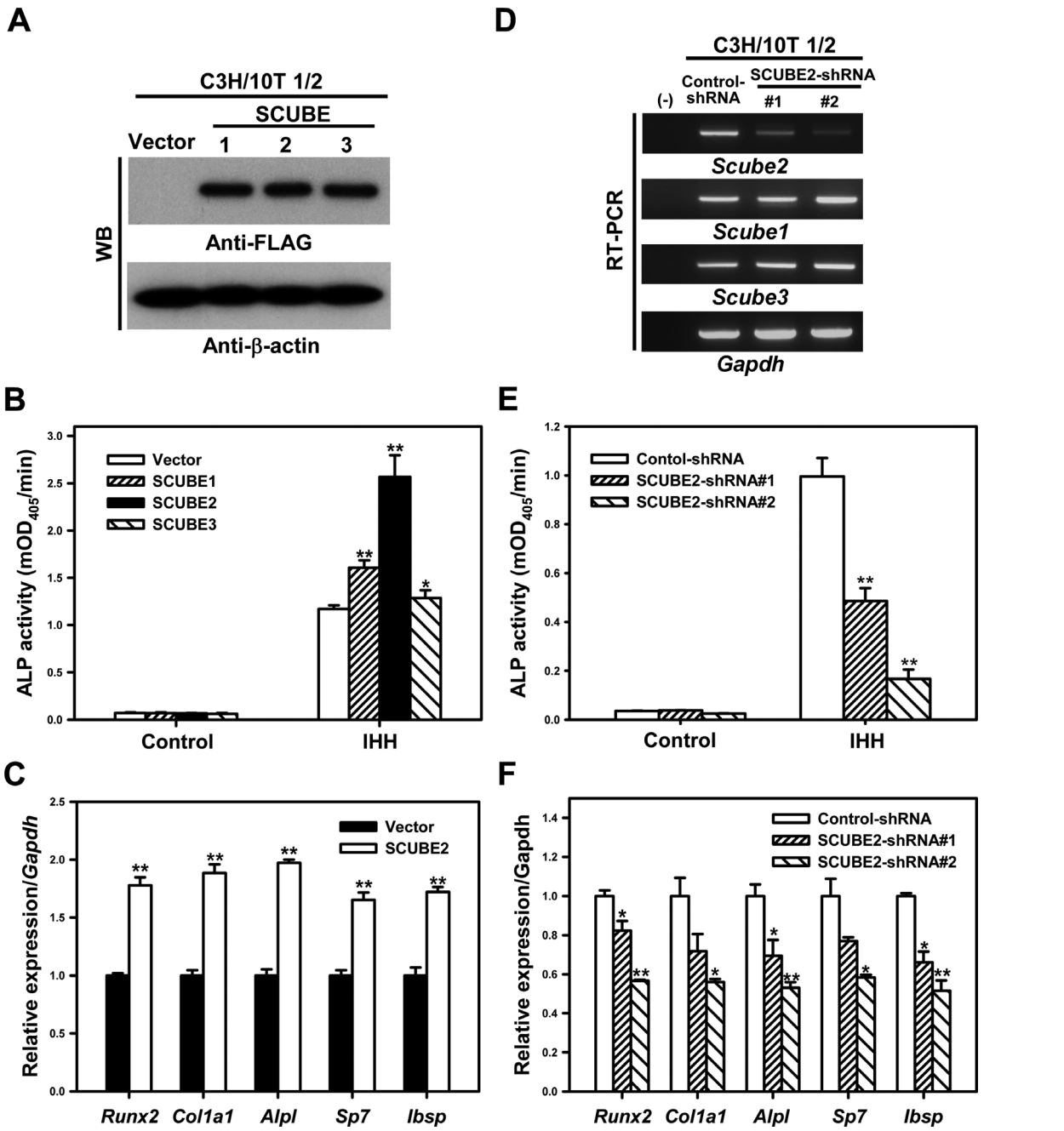

Fig. 3. SCUBE2 is involved in IHH-induced osteoblast differentiation. (*A*, *B*) Overexpression of SCUBE2 enhances IHH-induced osteoblast differentiation. C3H10T1/2 cells were engineered with the full-length SCUBE1–SCUBE3 expression vector or empty vector (Vector) by a lentiviral transduction system. Cell lysates from C3H10T1/2 vector or SCUBE1–SCUBE3-expressing cells were immunoblotted with antibodies for anti-FLAG (for SCUBE protein members expression) or β-actin (an internal control), respectively (*A*). C3H10T1/2 vector or SCUBE1–SCUBE3-expressing cells were cultured without or with IHH (800 ng/mL) for 7 days, then analyzed for ALP activity (an osteoblast differentiation marker). Data are mean ± SD. $^{**}p < 0.01$ compared with vector (*B*). (*D*, *E*) Knockdown of SCUBE2 reduced IHH-stimulated osteoblast differentiation in C3H10T1/2 cells. Endogenous SCUBE2 expression was suppressed by two independent SCUBE2-targeting shRNA lentiviruses (SCUBE2-shRNA #1 or #2) in C3H10T1/2 cells. A luciferase shRNA lentivirus was a negative control (Control-shRNA). The efficiency and specificity of mRNA knockdown for *Scube2* but not *Scube1* and *Scube3* was confirmed by RT-PCR because we lacked effective antibodies for Western blot analysis. *Gapdh* mRNA level was an internal control (*D*). C3H10T1/2 control-shRNA or SCUBE2-knockdown (SCUBE2 shRNA #1 and #2) cells were cultured without or with IHH (800 ng/mL) for 7 days. Cells were then analyzed for ALP activity. The experiments were performed three times in triplicate with similar results. Data are mean ± SD. $^{**}p < 0.01$ compared with control (*E*). (*C*, *F*) Quantitative real-time RT-PCR of osteoblastic marker genes in SCUBE2-overexpressing (*C*) or SCUBE2-knockdowned C3H10T1/2 cells (*F*). Expression of osteoblast marker genes *Runx2*, *Cola1*, *Alpl*, *Sp7*, and *Ibsp* was normalized to *Gapdh* mRNA level. The experiments were performed three times in triplicate with similar results. Data are mean ± SD. $^{*}p < 0.05$, $^{**}p < 0.01$. ALP = alkaline phosphatase; shRNA = short hairpin RNA; mOD_{405} = milli absorbance units at 405 nm; *Runx2* = Runt-related transcription factor 2; *Cola1* = type I collagen α1 chain; *Alpl* = alkaline phosphatase; *Sp7* = osterix; *Ibsp* = bone sialoprotein.

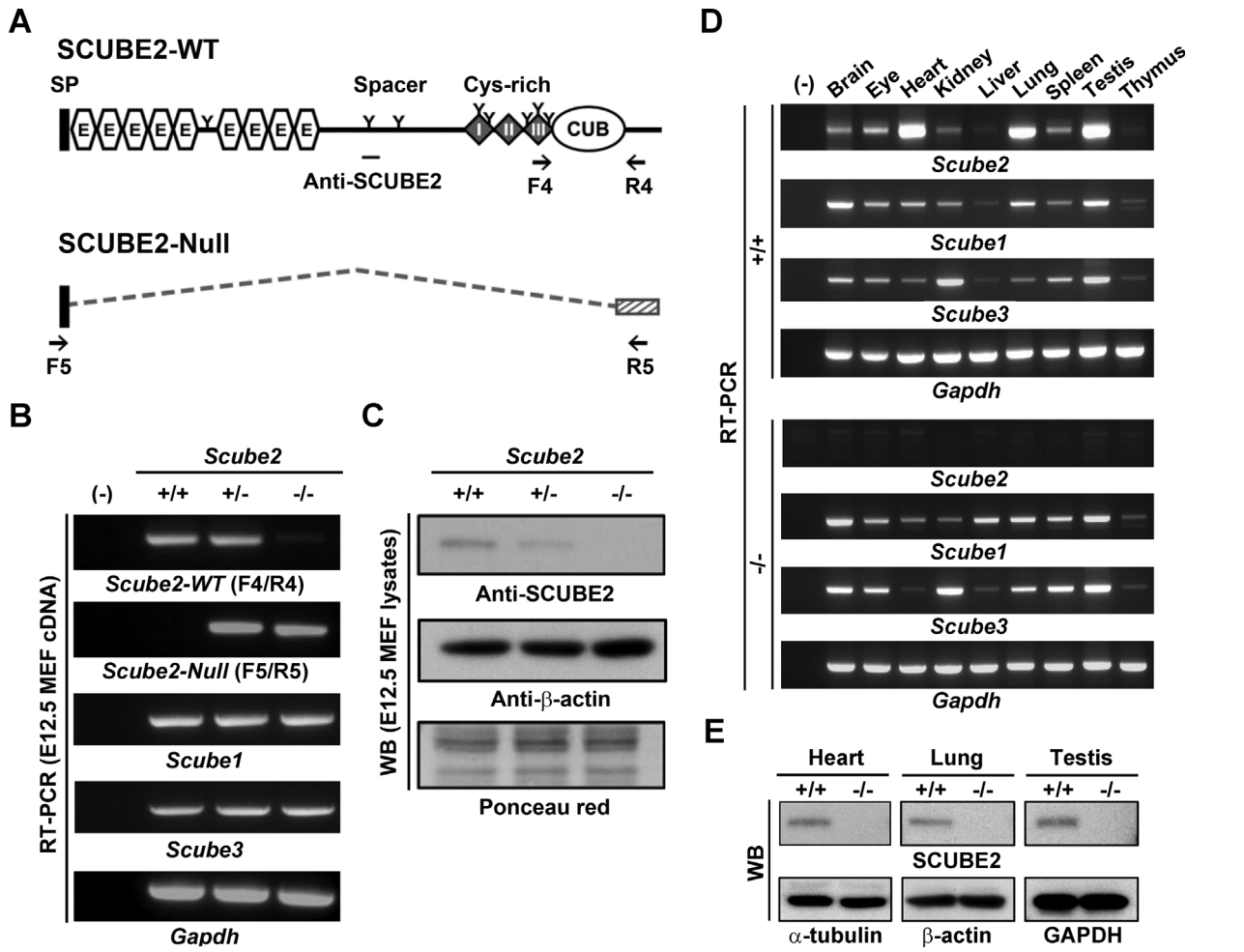

Fig. 4. Targeted disruption of *Scube2* at both mRNA and protein levels. (*A*) Graphic illustration of protein structure encoded by WT or null transcript. Locations of oligonucleotide primers used for RT-PCR and peptide antigen used to raise anti-SCUBE2 antibody for WB. Note that the null transcript joined the exons 1 and 22, which resulted in a frameshift to encode a polypeptide sequence (dashed line and hatched box) completely different from that of the WT locus. (*B*, *C*) The homozygous null mice lacked both mRNA and protein expression of *Scube2*. The first-strand cDNA (*B*) or protein lysates (*C*) from WT (+/+), heterozygous (+/–), and homozygous null (–/–) MEFs at day E12.5 was used for RT-PCR (primers F4 + R4 or F5 + R5 were used for WT or Null allele, respectively) or WB, respectively. Note that knockout of *Scube2* did not affect the expression of the two other *Scube* genes (*Scube1* and *Scube3*). Expression of *Gapdh* or β-actin was an internal control for RT-PCR or WB, respectively. Ponceau red staining of membranes confirmed the relative loading of total proteins in each sample. (*D*) Expression of *Scube* genes in major organs in +/+ and –/– adult animals. RT-PCR analysis of the expression of *Scube* genes. The first-stand cDNAs from several major organs of +/+ or –/– mice used for RT-PCR with primers specific for each *Scube* gene. Expression of *Gapdh* was an internal control. (*E*) Protein expression of SCUBE2 in +/+ and –/– adult mice. Protein lysates isolated from heart, lung, and testis in +/+ and –/– animals were immunoblotted with anti-SCUBE2 antibody. Expression of α-tubulin, β-actin, or GAPDH in heart, lung, or testis, respectively, was an internal control. WT = wild-type; WB = Western blot analysis; MEF = mouse embryonic fibroblast.

osteoblast differentiation), type I collagen α1 chain (*Col1a1*), alkaline phosphatase (*Alpl*), osterix (also named *Sp7*, a bone specific transcription factor essential for osteoblast differentiation and bone formation), and bone sialoprotein (*Bsp*, also known as integrin-binding sialoprotein *Ibsp*; a major structural protein of the bone matrix) was broadly in line with SCUBE2 overexpression or knockdown, respectively (Fig. 3*C*, *F*). Together, our data suggest that SCUBE2 exerts osteogenic action by modulating IHH-stimulated osteoblast differentiation, at least in vitro.

Generation of *Scube2* knockout (–/–) mouse strain

To further evaluate the osteogenic function of *Scube2* in vivo, we generated a new genetically altered mouse model lacking the functional *Scube2* gene (see Materials and Methods and Supporting Fig. S3). Mice homozygous for the WT (+/+) allele or the null (–/–) *Scube2* allele were obtained by interbreeding the heterozygous (+/–) offspring and verified by genomic PCR (Supporting Fig. S3D). In addition, RT-PCR analysis of the mRNA expression of *Scube2*-knockout (–/–) mouse embryonic fibroblasts (MEFs) at day E12.5 or an array of adult (8-week-old) organs followed by direct sequencing of the PCR product revealed completely deleted coding sequences for nine tandem epidermal growth factor-like domains, the spacer region, three cysteine-rich repeats, and the CUB domain (Fig. 4*A*, *B*, *D*). Furthermore, the mRNA expression of other *Scube* genes (*Scube1* and *Scube3*) remained unaltered between +/+ and –/– MEFs or organs (Fig. 4*B*, *D*). Consistent with the *Scube2*$^{-/-}$ mRNA

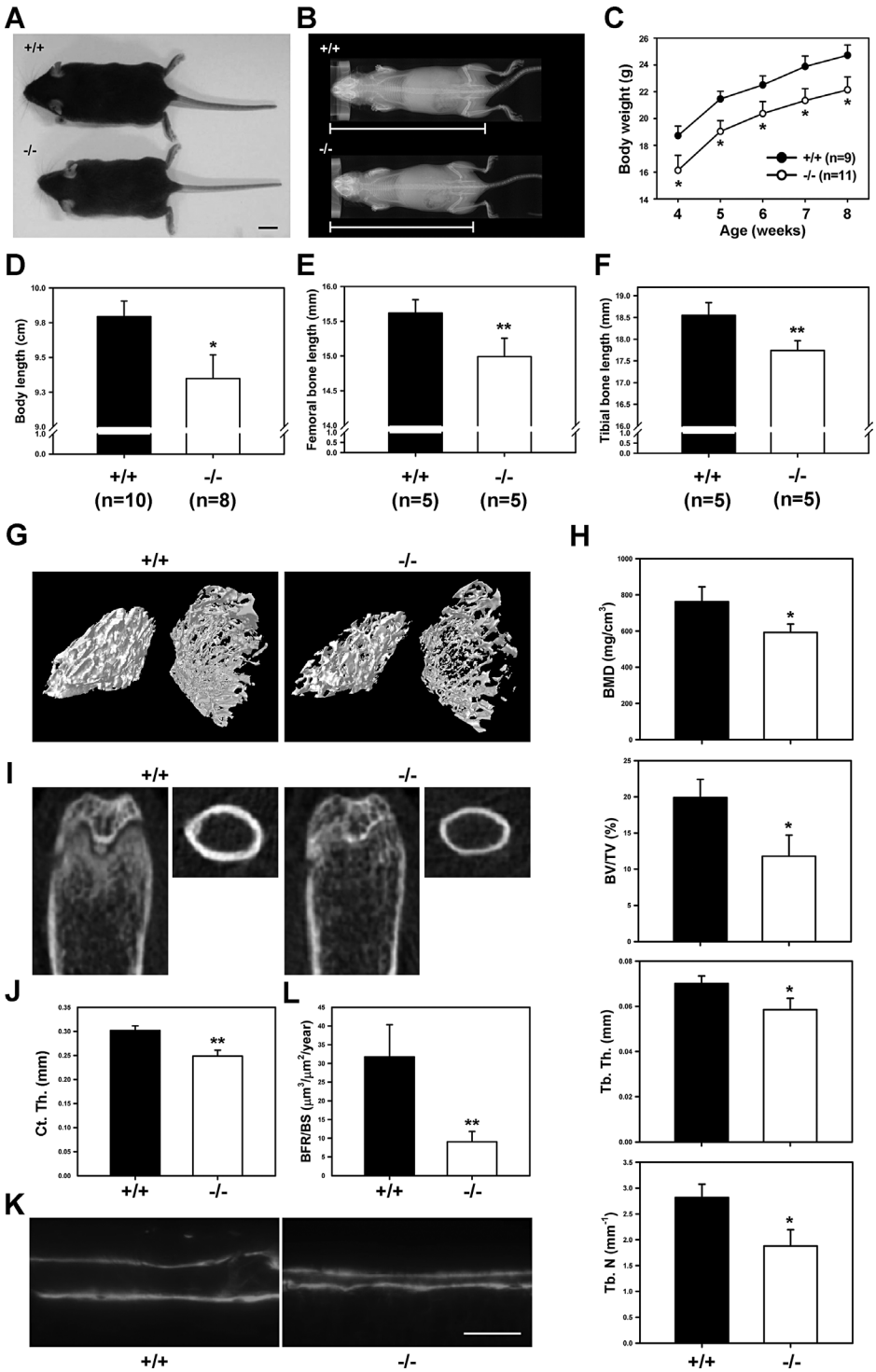

Fig. 5. Decreased body length and bone formation in –/– compared to +/+ mice. (*A*) Eight-week-old +/+ and knockout (–/–) mice. Representative photographs showing the size of –/– mice compared to +/+ littermates. Scale bar = 1 cm. (*B*) Whole-body radiographs. X-ray images of 8-week-old male +/+ and –/– mice. The nose-to-anus body lengths are marked. (*C*) Quantification of body weight from 4-week-old to 8-week-old +/+ ($n = 9$) and –/– ($n = 11$) mice. Data are mean ± SD. *$p < 0.05$. (*D–F*) Quantification of body (*D*), femur (*E*), and tibia (*F*) length of 8-week-old +/+ and –/– mice. Data are mean ± SD. *$p < 0.05$, **$p < 0.01$. (*G, I*) μCT of the distal femur and proximal tibia of 8-week-old +/+ and –/– mice. Reconstructed images of the proximal tibia and the distal femur (*G*) or the longitudinal view of the epiphyseal and metaphyseal regions (*I*, left panel) and the cross-sectional view of the cortical bone (mid-shaft) of the femur (*I*, right panel) are shown. (*H, J*) Quantification of mean BMD, BV/TV, Tb.Th, Tb.N, and Ct.Th. Data are mean ± SD ($n = 5$ in each group). *$p < 0.05$, **$p < 0.01$. (*K*) Double fluorochrome and calcein labeling of cortical femora of 6-week-old +/+ and –/– mice. Scale bar = 100 μm. (*L*) BFR/BS. Data are mean ± SD ($n = 5$ in each group). **$p < 0.01$. BMD = bone mineral density; BV/TV = bone volume per tissue volume; Tb. TH = trabecular thickness; Tb.N = trabecular number; Ct.Th = cortical thickness; BFR/BS = bone formation rate per bone surface.

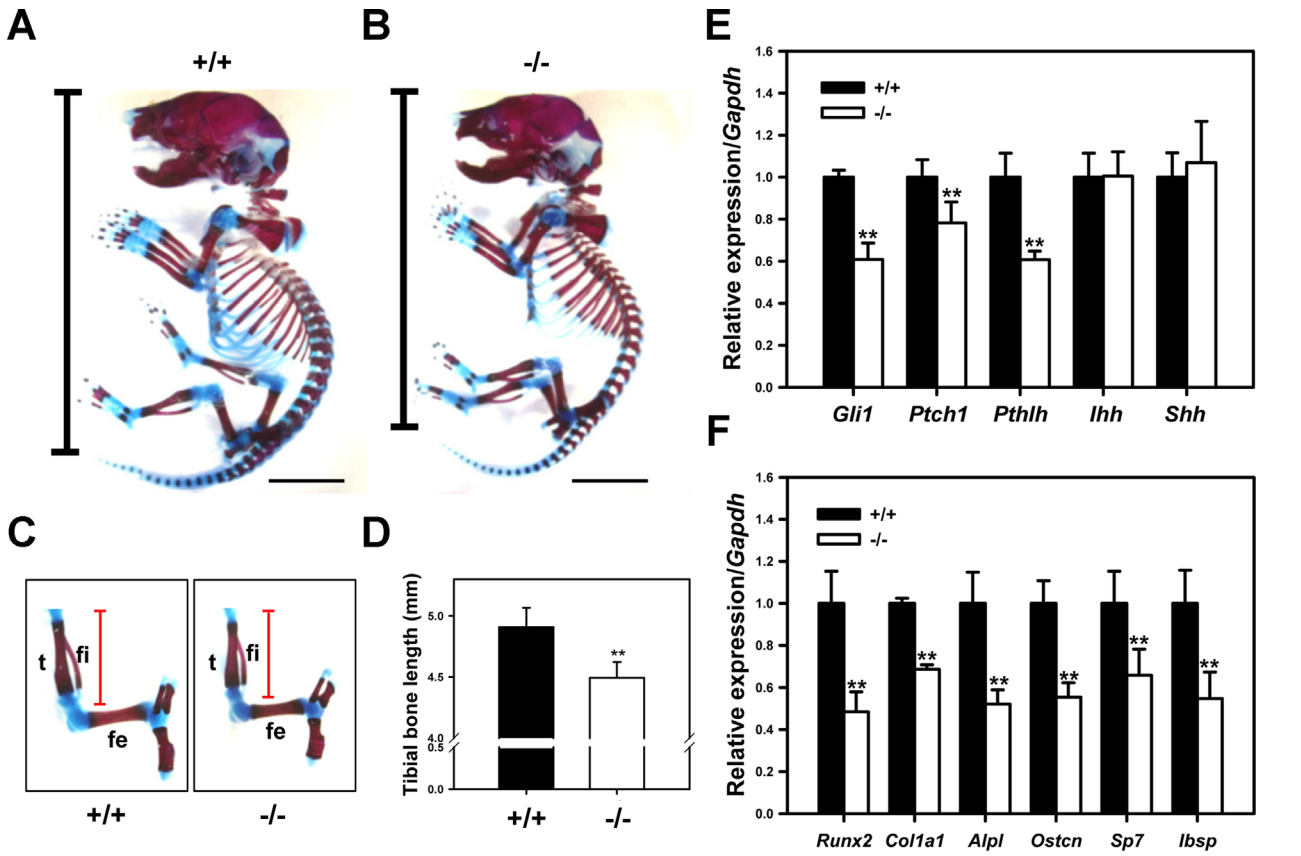

Fig. 6. Deficiency of *Scube2* impairs IHH-mediated signaling and endochondral bone formation. (*A*, *B*) Skeletons of +/+ and –/– newborns stained with Alizarin red (calcified tissue) and Alcian blue (cartilage). The nose-to-anus body lengths are marked. (*C*) Hindlimbs of +/+ and –/– animals stained with Alizarin red and Alcian blue. Tibial bone lengths are marked. (*D*) Quantification of tibial bone length. Data are mean ± SD ($n = 5$ in each group). $^{**}p < 0.01$. (*E*, *F*) Quantitative real-time RT-PCR of HH signaling components and osteogenic phenotype markers in long bones of hindlimbs from +/+ or –/– animals. Expression of HH pathway genes including *Ihh*, *Shh*, *Gli1*, *Ptch1*, and *Pthlh*. The latter three genes *Gli1*, *Ptch1*, *and Pthlh* are direct targets of HH signal activity (*E*). Expression of osteoblast marker genes *Runx2*, *Cola1*, *Alpl*, *Ostcn*, *Sp7*, and *Ibsp* was normalized to *Gapdh* mRNA level (*F*). Data are mean ± SD ($n = 6$ in each group). $^{**}p < 0.01$. fe = femur; t = tibia; fi = fibula. *Ihh* = Indian hedgehog; *Shh* = sonic hedgehog; *Pthlh* = parathyroid hormone-related protein; *Runx2* = Runt-related transcription factor 2; *Cola1* = type I collagen α1 chain; *Alpl* = alkaline phosphatase; *Ostcn* = osteocalcin; *Sp7* = osterix; *Ibsp* = bone sialoprotein.

transcript, SCUBE2 protein expression was completely eliminated in –/– MEFs (Fig. 4*C*) or adult –/– organs (Fig. 4*E*) including heart, lung, and testis where *Scube2* mRNA was highly expressed (Fig. 4*D*). Furthermore, immunohistochemical localization showed that anti-SCUBE2 staining was present in the periosteum, proliferative/prehypertrophic chondrocytes, and the trabecular region of +/+ tibia, whereas anti-SCUBE2 immunoreactivity was absent in –/– bones (Supporting Fig. S4). Together, we succeeded in producing *Scube2*-knockout animals that lacked the expression of functional SCUBE2 at both the mRNA and protein levels (Fig. 4). Mice with the –/– allele were backcrossed with WT C57BL/6 mice for at least six generations before phenotyping analyses.

Loss of endogenous soluble *Scube2* decreases the release and mobilization of HH ligands for long-range signaling

Previous reports showing the augmentation effect of SCUBE2 on the secretion of SHH ligand were mainly assessed by overexpression of SCUBE2 or the addition of exogenous SCUBE2 protein in a heterologous cell system.[23–25] We evaluated whether disruption of endogenous *Scube2* expression affected the release of SHH for long-range action in a "non-contact" co-culture (paracrine signaling) system. NIH/3T3 cells endogenously expressing HH protein were grown on six-well plates, and +/+ or –/– MEFs (infected with the empty or ectopic SCUBE2-carrying lentivirus) were co-cultured on Transwell inserts (Supporting Fig. S5A). This Transwell co-culture system allowed for the two cell populations to grow together in the same well but prevented direct cell–cell contact. Thus, soluble SCUBE2 proteins secreted from MEFs may diffuse through the pore of the membrane (3 μm) and act on NIH/3T3 cells in a paracrine fashion for the release of HH proteins. Two days after co-culturing, conditioned medium was collected and centrifuged at 100,000*g* for 2 hours to remove membranous remnants. The amount of secreted SHH ligand and its signaling activity were measured by ELISA and with Shh-LIGHT2 reporter cells, respectively.

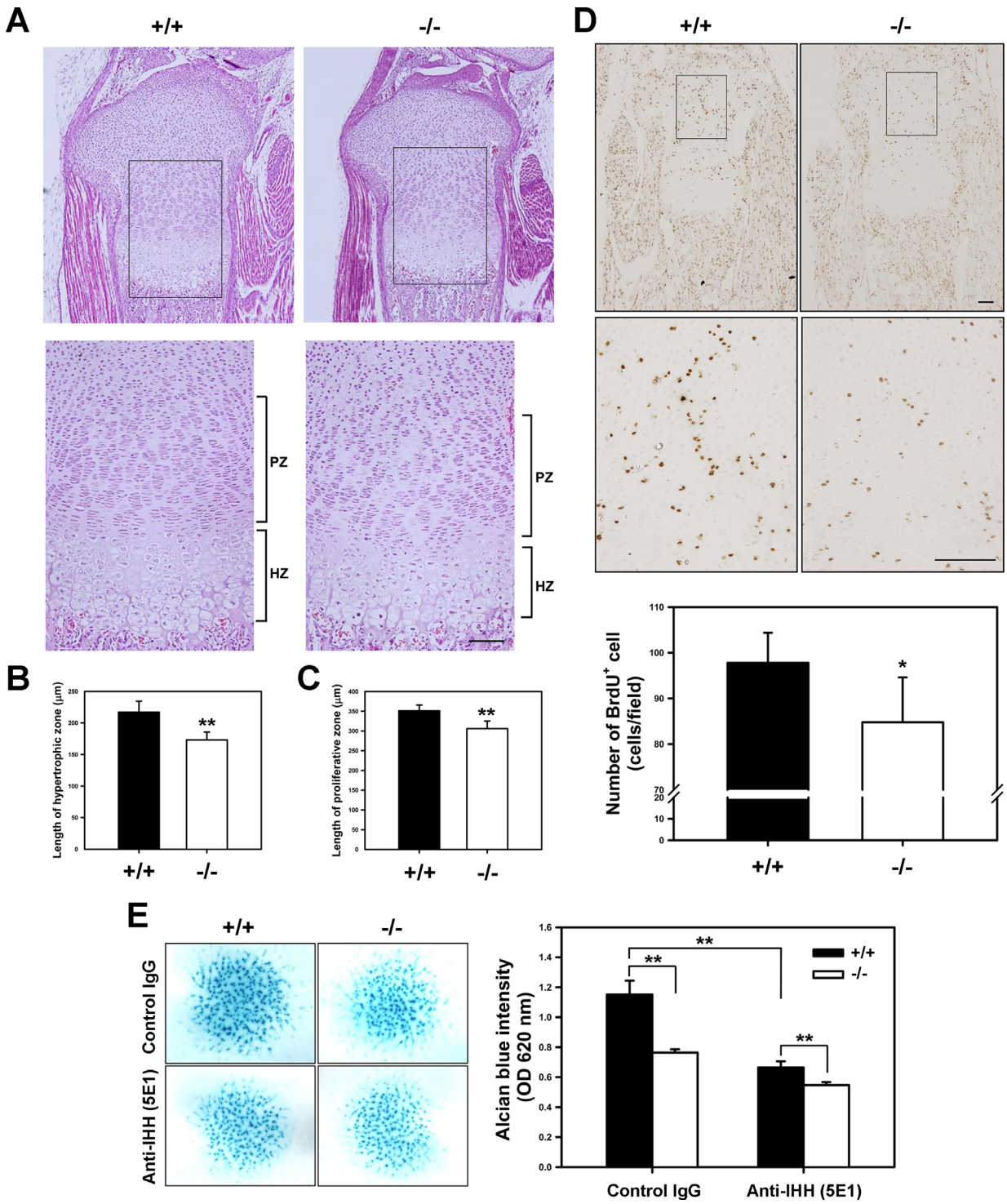

Fig. 7. Effects of *Scube2* knockout on the length of growth plates and chondrocyte proliferation and differentiation in the limbs by BrdU labeling or chondrocyte micromass cultures. (*A*) Hematoxylin-eosin staining of proximal tibia with PZ and HZ of growth-plate chondrocytes. Magnified views of the boxed regions are shown in the same columns. Scale bar = 100 μm. (*B*, *C*) Quantification of the length of the HZ (*B*) and PZ (*C*) in growth plates of +/+ and –/– animals. Data are mean ± SD ($n = 5$ in each group). **$p < 0.01$. (*D*) Immunohistochemistry of tibiae from BrdU-labeled +/+ and –/– neonatal pups using anti-BrdU antibody. Magnified views of the boxed periarticular regions are shown in the same columns. BrdU-positive cell number was counted and expressed as BrdU-positive cells/field in the periarticular regions of each section (low panel). *$p < 0.05$ ($n = 5$ animals in each genotype group). Scale bar = 100 μm. (*E*) Chondrocyte micromass cultures of mesenchymal cells from E11.5 +/+ and –/– mouse limbs treated with anti-IHH antibody (5E1) or isotype control IgG for 9 days (left panel). Alcian blue staining was quantified by solubilizing the sample in 6 M guanidine hydrochloride, followed by OD_{620} measurement by spectrophotometry (right panel). Data are mean ± SD. **$p < 0.01$. PZ = proliferative chondrocyte zone; HZ = hypertrophic chondrocyte zone; OD_{620} = optical density 620 nm.

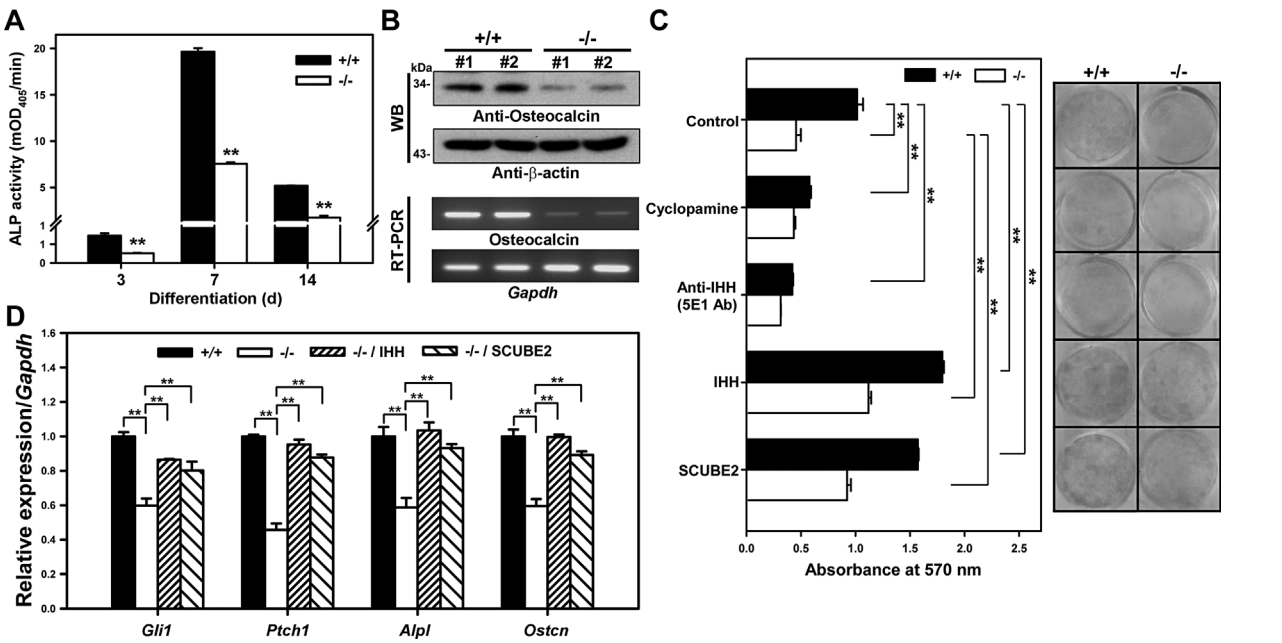

Fig. 8. Ex vivo osteogenic differentiation of +/+ or –/– BMSCs as assessed by ALP activity, osteocalcin expression, and Alizarin red staining. (*A*) ALP activity of +/+ and –/– BMSCs under osteoblast differentiation conditions at days 3, 7, and 14. The experiments were performed three times in triplicate with similar results. Data are mean ± SD. $^{**}p < 0.01$. (*B*) The protein and mRNA expression of osteocalcin in +/+ and –/– BMSCs under osteoblast differentiation conditions at day 7. Two independent BMSC cultures (#1 and #2) were used for Western blot and RT-PCR analyses. (*C*) Bone nodule formation in BMSC cultures under osteoblast differentiation conditions (right). Quantification of Alizarin red staining (left). The experiments were performed 3 times in triplicate with similar results. Data are mean ± SD. $^{**}p < 0.01$. (*D*) The mRNA expression of direct targets of HH signal activity (*Gli1* and *Ptch1*) and osteoblast marker genes (*Alpl* and *Ostcn*) in +/+ and –/– BMSCs under osteoblast differentiation conditions at day 7. The experiments were performed three times in triplicate with similar results. Data are mean ± SD. $^{**}p < 0.01$. BMSC = bone marrow stromal cell; ALP = alkaline phosphatase; mOD_{405} = milli absorbance units at 405 nm.

Loss of endogenous SCUBE2 in –/– MEFs clearly diminished soluble SCUBE2-mediated release of mature SHH from cultured cells and its long-range signaling activity (Supporting Fig. S5B and C, left panel). Most importantly, this defective activity of –/– MEFs could be rescued by lentivirus-mediated overexpression of SCUBE2 (Supporting Fig. S5B and C, right panel). Thus, deletion of endogenous soluble SCUBE2 reduced the release and mobilization of HH ligands for distal action.

Scube2 is dispensable for *Shh*-mediated developmental processes

Shh is essential for the development of the central nerve system, digit number and identity, and proper organogenesis of the heart, lung, and pancreas.[15] However, after heterozygous interbreeding, we produced mouse offspring with +/+, +/–, or –/– genotype with the expected Mendelian ratio; 0.96:2.1:0.94 ($n = 350$). Consistently, we observed no apparent abnormalities in –/– embryos at days E10.5 to 13.5 (Supporting Fig. S6A). In addition, the digit numbers and identities of forelimbs and hindlimbs appeared normal in –/– embryos (Supporting Fig. S6B). Furthermore, histological analyses of craniofacial tissues and heart, lung, and pancreas at E13.5 (Supporting Fig. S6C) or a number of adult organs including brain, eye, heart, lung, spleen, and testis (Supporting Fig. S7) confirmed normal development of these regions and organs in –/– mice as compared with +/+ littermates. Therefore, *Scube2* is not required for *Shh*-dependent developmental processes in vivo even though SCUBE2 has repeatedly been shown to augment the secretion and signaling of the dually lipid-modified SHH ligand in vitro.[1,23–25] Therefore, we examined the effects of *Scube2* on *Ihh*-dependent endochondral osteogenesis because *Scube2* mRNA expression was restricted to the perichondrial cells that differentiate into osteoblasts in the long bones[12] and SCUBE2 protein was expressed in the periosteal progenitor cells, proliferative/prehypertrophic chondrocytes as well as trabecular osteoblast cells (Supporting Fig. S4), and because SCUBE2 had the greatest effect on enhancing IHH signaling (Figs. 1 and 2) and promoted IHH-stimulated osteoblast differentiation in vitro (Fig. 3).

Deficiency of *Scube2* impairs IHH-mediated signaling and endochondral bone formation

In analyzing the –/– mouse phenotype, body size was lower in such mice as compared with their +/+ littermates (Fig. 5*A*). In addition, the general skeletal structure (skull, axial skeleton, ribs, pelvis, and long bones) of –/– mice, as revealed by whole-body radiography, appeared grossly normal but was smaller than +/+ animals (Fig. 5*B*). The shorter stature of –/– mice was seen at the time of weaning (3 weeks old) and persisted up to adulthood (Fig. 5*C*). Quantification of –/– and +/+ mice revealed reduced body weight (22.14 ± 0.98 versus 24.72 ± 0.79 g), nose-to-anus body length (9.25 ± 0.17 versus 9.79 ± 0.11 cm), femoral bone length (15.62 ± 0.19 versus 14.89 ± 0.26 mm), and tibial bone length (18.55 ± 0.29 vs 17.74 ± 0.23 mm) in adult mice (Fig. 5*C*–

F). In agreement with these findings, μCT of the metaphyseal regions of distal femur and proximal tibia demonstrated lower trabecular bone and reduced cortical thickness for –/– mice than +/+ littermates (Fig. 5*G*, *I*). Likewise, further histomorphometric analyses showed a significant reduction of trabecular volumetric bone mineral density (–22%), trabecular bone volume (–41%), trabecular thickness (–14%), trabecular number (–33%), and cross-sectional cortical thickness (–18%) in –/– animals compared to +/+ littermates (Fig. 5*H*, *J*). Double calcein and fluorochrome labeling revealed lower dynamic bone formation rate (–72%) in –/– mice than +/+ mice (Fig. 5*L*, *K*). Furthermore, double staining for ALP-positive osteoblasts and tartrate resistant acid phosphatase (TRAP)-positive osteoblasts showed that ALP-positive osteoblast cell number was significantly reduced whereas TRAP-positive osteoclast cell number remained unaltered in trabecular bone of the neonatal –/– tibias compared to +/+ controls (Supporting Fig. S8). Together, these results suggested that compromised endochondral ossification may be caused by defected bone formation rather enhanced resorption in *Scube2*-knockout mice.

At birth, –/– animals were invariably shorter than their +/+ littermates (Fig. 6*A*, *B*). Skeletons were stained with Alizarin red and Alcian blue to detect calcified tissues (hypertrophic cartilage and bone) and cartilage. Again, the skeletal elements of the –/– animals were present in the right position and in the right number. However, skeletogenesis was clearly abnormal, with all appendicular (the upper and lower limbs) and axial (the skull, the vertebral column, and the rib cage) skeletal elements smaller in –/– than +/+ mice (Fig. 6*A*–*D*). For instance, the length of tibia was slightly (10%) but significantly lower in –/– than +/+ animals (Fig. 6*C*, *D*).

To further confirm and quantify the HH signaling activity in –/– mice, microdissected long bones from the lower limbs from +/+ and –/– newborns were examined by quantitative real-time RT-PCR. HH ligand (*Ihh* and *Shh*) expression was similar between +/+ and –/– animals, but the levels of *Ihh* target genes *Gli1*, *Ptch1*, and parathyroid hormone-related protein (*Pthlh*) were greatly reduced in –/– long bones (Fig. 6*E*). In addition, the expression of osteogenic marker genes *Runx2*, *Col1a1*, *Alpl*, osteocalcin (*Ostcn*, the most specific marker of mature osteoblasts), osterix (*Sp7*), and bone sialoprotein (*Ibsp*) was markedly lower in –/– than +/+ long bones (Fig. 6*F*).

Histological analysis also revealed a marked reduction in the length of the proliferative (–20%) and hypertrophic (–15%) chondrocyte zone of –/– growth plates as compared with +/+ growth plates (Fig. 7*A*–*C*). In addition, we further analyzed chondrocyte proliferation in the +/+ and –/– limbs by BrdU labeling, and showed that chondrocyte proliferation (as measured by the number of BrdU-positive cells) in the tibiae was significantly reduced in the –/– mice compared to the +/+ animals (Fig. 7*D*). In addition, chondrocyte differentiation was evaluated by high-density micromass cell cultures of embryonic limb mesenchymal cells from +/+ and –/– embryos. Likewise, the –/– mesenchymal cells have a much less extent to undergo chondrogenic differentiation compared with +/+ mesenchymal cells. Notably, treatment with anti-IHH antibody (5E1) reduced chondrocyte differentiation in +/+ cells to the level comparable with that of –/– cells (Fig. 7*E*). Together, these data suggest that *Scube2* plays a critical role in *Ihh*-dependent endochondral bone formation through regulating the osteogenic differentiation (Fig. 6) as well as the chondrogenic differentiation and proliferation (Fig. 7).

Ex vivo differentiation of osteoprogenitors supports that *Scube2* acts as an enhancer of osteoblastogenesis

To further examine whether +/+ and –/– mice differed in the ability to undergo osteoblast differentiation, BMSCs from +/+ and –/– mice were cultured in osteogenic differentiation media, and the degree of ex vivo osteogenic differentiation was evaluated by osteoblast phenotype markers including ALP activity, osteocalcin expression, or Alizarin red staining for matrix mineralization. ALP activity increased over time and peaked at day 7 in BMSC cultures for both genotypes, with lower level for –/– than +/+ cultures on days 3, 7, and 14 (by 36%, 38%, and 34%, respectively; Fig. 8*A*). Similarly, both mRNA and protein levels of osteocalcin were greatly reduced in –/– BMSC culture (>90%) (Fig. 8*B*), as was Alizarin red staining (~55%) as compared with +/+ BMSC culture (Fig. 8*C*, top). Of note, inactivation of *Scube2* does not affect the proliferation rate of –/– osteoprogenitor cells compared to +/+ cells (Supporting Fig. S9). Therefore, inactivation of *Scube2* impeded the osteogenic differentiation but not proliferation of BMSCs, analogous to the in vivo –/– phenotype (Figs. 5–7).

To further investigate the involvement of IHH signaling in *Scube2*-mediated osteogenic differentiation, we used loss-of-function and gain-of-function experiments specifically targeting the IHH signal pathway. We first pharmacologically blocked IHH signaling in the ex vivo system described above in Fig. 8*A* with a HH signaling inhibitor (cyclopamine) or by direct IHH blocking with the neutralizing monoclonal antibody 5E1.[37] Treatment with these IHH signaling inhibitors greatly decreased osteogenic calcification, as measured by Alizarin red staining, in +/+ BMSC cultures to the level of –/– BMSCs under osteogenic differentiation conditions (Fig. 8*C*, middle), so IHH signaling was required for +/+ BMSCs to differentiate into mature osteoblasts. Most importantly, supplementation with IHH or soluble SCUBE2 protein further enhanced osteogenic maturation in +/+ BMSCs and completely restored matrix mineralization in –/– BMSC culture (Fig. 8*C*, bottom). In addition, similar results were obtained when the *Scube2*-floxed osteoprogenitor cells were isolated and inactivated by Cre-mediated excision of the floxed alleles, excluding the potential involvement of unknown systemic factors in defected osteogenic differentiation (Supporting Fig. S10). Consistent with these findings, –/– BMSC osteogenic culture showed reduced IHH signal activity (decreased *Gli1* and *Ptach1* mRNA expression) and impaired osteogenic differentiation (reduced *Alpl* and *Ostcn* expression); such defects could be rescued by the exogenous addition of IHH and soluble SCUBE2 protein (Fig. 8*D*). These data demonstrate that IHH signaling is indeed involved in *Scube2*-mediated osteoblast differentiation and bone matrix production in +/+ BMSC osteogenic cultures.

Discussion

Zebrafish genetic[8–10] and biochemical studies[1,23–25] have implicated SCUBE2 in modulating SHH signaling activity for proper development of slow muscle; however, the precise functions of mammalian SCUBE2 in regulating the activity of other HH ligands such as IHH or DHH and the developmental significance of the SCUBE2-mediated secretion and mobilization of SHH signals remain poorly understood. In this study, we first systemically examined the effect of each SCUBE member on signaling activity of all three HH ligands and found that SCUBE2 had the greatest effect on promoting IHH signaling in a Gli-

driven reporter cell line (Figs. 1 and 2). In addition, gain and loss-of-function experiments suggested that SCUBE2 is critical for IHH-stimulated osteogenic differentiation in mouse mesenchymal progenitor cells (Fig. 3). Further knockout studies showed that loss of *Scube2* impaired endochondral bone formation and IHH-induced osteoblast differentiation in –/– BMSC cultures (Figs. 5–8). In agreement with the reduction of growth-plate chondrocytes in –/– bones, our BrdU labeling and chondrocyte micromass culture assays further revealed that *Scube2* is also involved in the regulation of *Ihh*-dependent chondrocyte differentiation and proliferation (Fig. 7). Therefore, it is tempting to speculate that SCUBE2 protein expressed in perichondrial cells may be secreted and modulate the prehypertrophic chondrocyte-derived IHH signals by facilitating the release and mobilization of IHH for differentiation into osteoblasts during endochondral bone formation. Together, our results agree with in vitro studies,[1,23–25] revealing that mammalian SCUBE2 can act cell-autonomously and non-cell-autonomously to coordinate skeletogenesis by fine-tuning IHH signal activities in prechondrium/osteoblasts or chondrocytes for their differentiation and/or proliferation.

However, the shortcoming of the global mutant mice is that these skeletal phenotype including overall reduced length and weight of mutant mice as well as their smaller growth plates could be results of an unknown systemic *Scube2*-deficient effect, rather than being the direct consequence of loss of *Scube2* in cells of the osteoblast and/or chondrocyte lineages. Further investigations by using the osteoblast-specific (Col1a1-Cre) and/or chondrocyte (Col2a1-Cre)-specific *Scube2*-knockout mouse lines are warranted to validate the relative contribution of osteoblasts or chondrocytes on the observed bone phenotypes.

Of note, the *Scube2*-deficient embryos appeared normal in *Shh*-dependent developmental processes, including the development of the central nerve system, digit number, and identity, and organogenesis of the heart, lung, and pancreas,[15] so SCUBE2-mediated release of SHH ligand for distant signaling is dispensable for normal development and survival and points to a possible redundant role of other *Scube* genes (*Scube1* or *Scube3*) in maintaining proper SHH signal intensities during embryonic development in *Scube2*-deficient mice. Double or triple knockout of these *Scube* genes may be required to further elucidate their cooperative roles in *Shh*-induced developmental processes.

Alternatively, remaining SHH ligand released or transported by SCUBE2-independent molecules such as the family of metalloproteases, a disintegrin and metalloprotease domain (ADAM),[38,39] or Dispatched, a transporter-like protein with a role in the secretion of lipid-modified HH signals,[40] may be sufficient for delicate *Shh*-mediated developmental processes in *Scube2*-deficient embryos. Similarly, such residual SCUBE2-independent secretion or solubilization of the IHH signal may account for the modest osteogenic and chondrogenic phenotypes observed in –/– skeletons.

One interesting observation is that although SCUBE family members share an overall similar protein domain organization, including signal peptide sequence, epidermal growth factor-like repeat, spacer-region, cysteine-rich, and CUB domains, SCUBE2 is the most potent enhancer of IHH signals (Figs. 1–3). Nonetheless, the amino acid sequences of the spacer region and the distribution of potential N-linked glycan sites are divergent and distinctive in SCUBE2 as compared with SCUBE1 or SCUBE3. These unique features of SCUBE2 might determine its specific targeting to membrane lipid rafts that contain dually lipidated HH ligands and its signaling component PTCH1 in these microdomains,[1,41,42] and contribute to its uppermost activity on promoting IHH secretion or signaling. However, further investigations are needed to verify this hypothesis.

In summary, our results demonstrate that SCUBE2 plays a critical role in modulating IHH signals during endochondral ossification. Apart from its expression in multiple sites of endochondral skeletal structures, *Scube2* transcript was also found in a wide spectrum of developing tissues including neuroectoderm, craniofacial region, heart and vasculature.[7,12] Further studies are required to fully elucidate the subtle involvement of *Scube2* in these developing tissues and its roles in HH-related human pathologies such as skeletal disorders and cancer progression.

Disclosures

All authors state that they have no conflicts of interest.

Acknowledgments

This work was supported by grants from the Ministry of Science and Technology of Taiwan (MOST 103-2325-B-001-004 and MOST 102-2320-B-001-015-MY3). RNAi reagents were obtained from the National RNAi Core Facility at the Institute of Molecular Biology/Genomic Research Center, Academia Sinica, supported by National Core Facility Program for Biotechnology Grants from the National Science Council (NSC), Taiwan (NSC 100-2319-B-001-002). We thank the technical services provided by the Transgenic Mouse Model Core Facility of the National Core Facility Program for Biotechnology, NSC, and the Gene Knockout Mouse Core Laboratory of the National Taiwan University Center of Genomic Medicine. In addition, we thank the Taiwan Mouse Clinic (MOST 103-2325-B-001-015), which is funded by the National Research Program for Biopharmaceuticals, NSC, Taiwan for technical support in bone phenotyping analyses.

Authors' roles: YCL, YTY, and RBY designed the research. SRR provided critical reagents. YCL and YTY performed the research. YCL, YTY, and RBY analyzed the data. YCL and RBY wrote the manuscript.

References

1. Tsai MT, Cheng CJ, Lin YC, et al. Isolation and characterization of a secreted, cell-surface glycoprotein SCUBE2 from humans. Biochem J. 2009;422:119–28.
2. Yang RB, Ng CK, Wasserman SM, et al. Identification of a novel family of cell-surface proteins expressed in human vascular endothelium. J Biol Chem. 2002;277:46364–73.
3. Lin YC, Chen CC, Cheng CJ, Yang RB. Domain and functional analysis of a novel breast tumor suppressor protein, SCUBE2. J Biol Chem. 2011;286:27039–47.
4. Lin YC, Lee YC, Li LH, Cheng CJ, Yang RB. Tumor suppressor SCUBE2 inhibits breast-cancer cell migration and invasion through the reversal of epithelial-mesenchymal transition. J Cell Sci. 2014;127:85–100.
5. Gal P, Zavodszky P. Structure and function of the serine-protease subcomponents of C1: protein engineering studies. Immunobiology. 1998;199:317–26.
6. Grimmond S, Larder R, Van Hateren N, et al. Cloning, mapping, and expression analysis of a gene encoding a novel mammalian EGF-related protein (SCUBE1). Genomics. 2000;70:74–81.
7. Grimmond S, Larder R, Van Hateren N, et al. Expression of a novel mammalian epidermal growth factor-related gene during mouse neural development. Mech Dev. 2001;102:209–11.

8. Woods IG, Talbot WS. The you gene encodes an EGF-CUB protein essential for Hedgehog signaling in zebrafish. PLoS Biol. 2005;3:e66.
9. Kawakami A, Nojima Y, Toyoda A, et al. The zebrafish-secreted matrix protein you/scube2 is implicated in long-range regulation of hedgehog signaling. Curr Biol. 2005;15:480–8.
10. Hollway GE, Maule J, Gautier P, et al. Scube2 mediates Hedgehog signalling in the zebrafish embryo. Dev Biol. 2006;294:104–18.
11. Wu BT, Su YH, Tsai MT, et al. A novel secreted, cell-surface glycoprotein containing multiple epidermal growth factor-like repeats and one CUB domain is highly expressed in primary osteoblasts and bones. J Biol Chem. 2004;279:37485–90.
12. Xavier GM, Cobourne MT. Scube2 expression extends beyond the central nervous system during mouse development. J Mol Histol. 2011;42:383–91.
13. Kronenberg HM. The role of the perichondrium in fetal bone development. Ann N Y Acad Sci. 1997;1116:59–64.
14. Colnot C, Lu C, Hu D, Helms JA. Distinguishing the contributions of the perichondrium, cartilage, and vascular endothelium to skeletal development. Dev Biol. 2004;269:55–69.
15. McMahon AP, Ingham PW, Tabin CJ. Developmental roles and clinical significance of hedgehog signaling. Curr Top Dev Biol. 2003;53:1–114.
16. Hooper JE, Scott MP. Communicating with Hedgehogs. Nat Rev Mol Cell Biol. 2005;6:306–17.
17. St-Jacques B, Hammerschmidt M, McMahon AP. Indian hedgehog signaling regulates proliferation and differentiation of chondrocytes and is essential for bone formation. Genes Dev. 1999;13:2072–86.
18. Chung UI, Schipani E, McMahon AP, Kronenberg HM. Indian hedgehog couples chondrogenesis to osteogenesis in endochondral bone development. J Clin Invest. 2001;107:295–304.
19. Long F, Chung UI, Ohba S, et al. Ihh signaling is directly required for the osteoblast lineage in the endochondral skeleton. Development. 2004;131:1309–18.
20. Mak KK, Kronenberg HM, Chuang PT, Mackem S, Yang Y. Indian hedgehog signals independently of PTHrP to promote chondrocyte hypertrophy. Development. 2008;135:1947–56.
21. Long F, Zhang XM, Karp S, Yang Y, McMahon AP. Genetic manipulation of hedgehog signaling in the endochondral skeleton reveals a direct role in the regulation of chondrocyte proliferation. Development. 2001;128:5099–108.
22. Maeda Y, Nakamura E, Nguyen MT, et al. Indian Hedgehog produced by postnatal chondrocytes is essential for maintaining a growth plate and trabecular bone. Proc Natl Acad Sci U S A. 2007;104:6382–7.
23. Creanga A, Glenn TD, Mann RK, et al. Scube/You activity mediates release of dually lipid-modified Hedgehog signal in soluble form. Genes Dev. 2012;26:1312–25.
24. Tukachinsky H, Kuzmickas RP, Jao CY, Liu J, Salic A. Dispatched and scube mediate the efficient secretion of the cholesterol-modified hedgehog ligand. Cell Rep. 2012;2:308–20.
25. Jakobs P, Exner S, Schurmann S, et al. Scube2 enhances proteolytic Shh processing from the surface of Shh-producing cells. J Cell Sci. 2014;127:1726–37.
26. Lai LP, Mitchell J. Indian hedgehog: its roles and regulation in endochondral bone development. J Cell Biochem. 2005;96:1163–73.
27. Taipale J, Chen JK, Cooper MK, et al.. Effects of oncogenic mutations in Smoothened and Patched can be reversed by cyclopamine. Nature. 2000;406:1005–9.
28. Deglon N, Tseng JL, Bensadoun JC, et al. Self-inactivating lentiviral vectors with enhanced transgene expression as potential gene transfer system in Parkinson's disease. Hum Gene Ther. 2000;11:179–90.
29. Root DE, Hacohen N, Hahn WC, Lander ES, Sabatini DM. Genome-scale loss-of-function screening with a lentiviral RNAi library. Nat Methods. 2006;3:715–9.
30. Nishimura R, Hata K, Harris SE, Ikeda F, Yoneda T., Core-binding factor alpha 1 (Cbfa1) induces osteoblastic differentiation of C2C12 cells without interactions with Smad1 and Smad5. Bone. 2002;31:303–12.
31. O'Gorman S, Dagenais NA, Qian M, Marchuk Y. Protamine-Cre recombinase transgenes efficiently recombine target sequences in the male germ line of mice but not in embryonic stem cells. Proc Natl Acad Sci U S A. 1997;94:14602–7.
32. Sontag W., An automatic microspectrophotometric scanning method for the measurement of bone formation rates in vivo. Calcif Tissue Int. 1980;32:63–8.
33. McLeod MJ. Differential staining of cartilage and bone in whole mouse fetuses by Alcian blue and Alizarin red S. Teratology. 1980;22:299–301.
34. Maniatopoulos C, Sodek J, Melcher AH. Bone formation in vitro by stromal cells obtained from bone marrow of young adult rats. Cell Tissue Res. 1988;254:317–30.
35. Shimoyama A, Wada M, Ikeda F, et al. Ihh/Gli2 signaling promotes osteoblast differentiation by regulating Runx2 expression and function. Mol Biol Cell. 2007;18:2411–8.
36. Nakamura T, Aikawa T, Iwamoto-Enomoto M, et al. Induction of osteogenic differentiation by hedgehog proteins. Biochem Biophys Res Commun. 1997;237:465–9.
37. Wang W, Lian N, Ma Y, et al.. Chondrocytic Atf4 regulates osteoblast differentiation and function via Ihh. Development. 2012;139:601–11.
38. Ohlig S, Farshi P, Pickhinke U, et al. Sonic hedgehog shedding results in functional activation of the solubilized protein. Dev Cell. 2011;20:764–74.
39. Dierker T, Dreier R, Petersen A, Bordych C, Grobe K., Heparan sulfate-modulated, metalloprotease-mediated sonic hedgehog release from producing cells. J Biol Chem. 2009;284:8013–22.
40. Burke R, Nellen D, Bellotto M, et al. Dispatched, a novel sterol-sensing domain protein dedicated to the release of cholesterol-modified hedgehog from signaling cells. Cell. 1999;99:803–15.
41. Rietveld A, Neutz S, Simons K, Eaton S. Association of sterol- and glycosylphosphatidylinositol-linked proteins with Drosophila raft lipid microdomains. J Biol Chem. 1999;274:12049–54.
42. Traiffort E, Moya KL, Faure H, Hassig R, Ruat M. High expression and anterograde axonal transport of aminoterminal sonic hedgehog in the adult hamster brain. Eur J Neurosci. 2001;14:839–50.